Polymer Journal
https://doi.org/10.1038/s41428-024-00895-9

ORIGINAL ARTICLE

Melt adsorption of poly(*tert*-butyl methacrylate) and poly(ethyl methacrylate) on silica studied with chip nanocalorimetry

Minato Ishihara[1] · Tomoya Watanabe[1] · Toyoaki Hirata[2] · Takashi Sasaki[1]

Received: 10 October 2023 / Revised: 10 January 2024 / Accepted: 19 January 2024

Abstract

Irreversible adsorption of polymer chains from a melt on a substrate surface can be strongly affected by interfacial interactions. In this study, we examined the adsorption of two polymers, poly(*tert*-butyl methacrylate) (PtBMA) and poly(ethyl methacrylate) (PEMA), on a silica surface at temperatures above their glass transition temperatures. The degree of adsorption $\gamma(t)$ over time was evaluated with variations of storage heat capacity determined with alternating current chip nanocalorimetry (in-situ measurement of a buried interface). $\gamma(t)$ revealed two-step profiles for both polymers. At the second stage of adsorption (regime II), the slope of a plot of $\gamma(t)$ vs. log t increased as adsorption proceeded; this trend has not been reported for other polymers and may be characteristic of the present polymers. The trend observed in regime II suggested that the unadsorbed free chains near the interface became less mobile and were incorporated into the adsorbed layer via interactions with the tails of the chains directly attached to the substrate surface. The increasing slope in regime II was more prominent for PtBMA than for PEMA. In addition, a difference was observed for PtBMA and PEMA in the atomic force microscopy images of the exposed adsorption layer surfaces.

Introduction

Because the mechanism has not been fully elucidated, the adsorption of polymers from the melt onto substrate surfaces has attracted much attention from the soft matter community. The adsorbed layers often play important roles in controlling the properties of composite materials, such as the glass transition temperature [1–4], viscosity [5, 6], dewetting [7–9], thermal expansion [10], and crystallization [11–13]. Thus, elucidation of the mechanism could provide guidelines for the development of adhesion technology and molecular designs for various composite materials. The adsorption of polymers as an interfacial phenomenon should be understood on the basis of the chemistry of the materials at the molecular level.

The conformations of polymer chains attached to a surface are typically characterized as trains, loops, and tails, which date back to Jenkel and Rumbach in 1951 [14]. Guiselin discovered a method for preparing irreversibly adsorbed chains with a thought experiment [15], which is currently used as a fundamental procedure to study polymer adsorption. Then, it was revealed that the irreversibly-adsorbed polymer consists of two stable nanolayers: a flattened layer and an interfacial sublayer [5, 7, 9, 16, 17]. Additionally, many previous studies revealed that the adsorption rate depends on the temperature [1, 18–21], polymer/substrate interactions [17, 22, 23], and average molecular weight of the polymer [1, 18, 19].

The nature of melt adsorption was studied based on thermodynamic insights. It was reported that the temperature dependence of the adsorption rate is one of the most important aspects. For example, Napolitano et al. reported that when films were annealed at a temperature above the glass transition temperature T_g ($T_g + 50$ K), the amount of polystyrene (PS) adsorbed increased until it reached saturation at 3×10^4 s. Conversely, when the annealing temperature was low (T_g(bulk) + 15 K), adsorption occurred over several months [1]. Other groups reported the same

Supplementary information The online version contains supplementary material available at https://doi.org/10.1038/s41428-024-00895-9.

✉ Takashi Sasaki
sasakita@u-fukui.ac.jp

[1] Department of Materials Science and Engineering, University of Fukui, Fukui 9108507, Japan

[2] Department of Frontier Fiber Technology and Science, University of Fukui, Fukui 9108507, Japan

Published online: 15 February 2024

tendencies for various polymers [18–21]. This temperature dependence may be interpreted as follows: annealing at high temperature provides high polymer chain mobility at the interface, which promotes irreversible adsorption. However, the desorption process must be considered to understand the mechanism for irreversible adsorption. One may consider that at higher temperatures, the net adsorption rate should decrease because the desorption process is activated. Monnier et al. qualitatively evaluated the desorption energy of an adsorbed polymer chain with fast scanning calorimetry [24]. The desorption signal appeared at a much higher temperature than the adsorption temperature. Thus, irreversible adsorption may occur in a temperature range much lower than the desorption peak, where adsorption overcomes desorption.

The polymer/substrate interactions at the interface strongly affect the adsorption rate. Davis et al. reported that the temperature dependence of the adsorption rate was stronger for poly(methyl methacrylate) (PMMA) than for PS [22]. It was suggested that the hydrogen bonds between the carbonyl groups of PMMA and the hydroxyl groups of the silica surface led to a higher density of adsorbed chains, and this effect of hydrogen bonding was stronger than that of van der Waals interactions. In addition, Fujii et al. revealed that the amount of PS adsorbed from a melt was greater on an H-Si surface than on a SiO_x-Si surface after the same annealing time [25]. Notably, the mobility of the polymer played a crucial role because the adsorption process involved polymer chain dynamics [26–37]. To the best of our knowledge, there is no direct evidence of a correlation between the conformations of surface-bound chains and the adsorption rate. In general, the polymer chain mobility depends strongly on the chemical structure. Thus, it is important to investigate how the rigidity of a polymer alters its adsorption behavior.

Furthermore, there are still questions regarding the methods used to measure melt adsorption. As noted by Michael et al., there is no enthalpy change associated with adsorption from the melt. Using established techniques, such as atomic force microscopy (AFM) [9, 38], X-ray reflectivity [5, 7, 16, 17], and ellipsometry [3, 38–41], the adsorption kinetics were investigated by evaluating the thickness of the adsorbed layer as a function of the annealing time, and a solvent washing procedure was required to expose the adsorbed layer. The solvent may cause some rearrangement of the polymer chains; however, the details have not been elucidated.

We previously applied alternating current (AC) chip nanocalorimetry to investigate adsorption kinetics at a buried interface (without solvent washing) [42]. This technique allows real-time measurement of polymer adsorption onto the silica surface of a chip sensor. An advantage of chip nanocalorimetry is that nonconductive substrates such as silica can be used. With AC chip calorimetry, we investigated the time evolution for the amount of adsorbed polymer, which increased as a function of the annealing time.

In this study, we investigated the adsorption of two polymers with different side groups, poly(ethyl methacrylate) (PEMA) and poly(*tert*-butyl methacrylate) (PtBMA), with AC chip calorimetry. These two polymers have the same backbone structure and are expected to have similar chemical properties but different rigidities owing to their different side groups. We also investigated temporal evolution of the morphologies of the adsorbed layers via AFM.

Materials and methods

Materials

PtBMA ($M_w = 680$ kDa) and PEMA ($M_w = 250$ kDa) were purchased from Scientific Polymer Products (Ontario, NY, USA). The polymer parameters are summarized in Table 1. The glass transition temperatures (T_g) of PtBMA and PEMA were determined with differential scanning calorimetry (DTG-60, Shimadzu, Kyoto, Japan). The measurements were performed at a heating rate 20 K min^{-1} over the temperature range from 333 to 433 K under a nitrogen atmosphere, and the T_g was evaluated from the second heating trace. Toluene (Kanto Chemical Co., Tokyo, Japan) was used as the polymer solvent. The radius of gyration for a Gaussian polymer chain R_g was estimated with a monomer unit length of 0.25 nm.

Differential AC chip calorimetry

A chip calorimeter (Xensor Integration XI-39390, Delfgauw, Netherlands) was used for nanocalorimetry. The polymer film was mounted on the chip sensor as follows. As a pretreatment, the active area of the chip sensor was washed three times with toluene. It was subsequently annealed at 433 K for 2 h [43]. PtBMA films (approximately 70 nm in thickness) were spun at 1000 rpm for 30 s from a 1.0 wt% PtBMA/toluene solution onto glass substrates. The film thickness was measured with a laser interferometer (Filmetrics F20, Yokohama, Japan). These films were cut into pieces measuring approximately 2 × 3

Table 1 Parameters of the polymers used in this study

Polymer	M_w/kDa	T_g/K	R_g[a]/nm
PtBMA	680	380	7.1
PEMA	250	349	4.8

[a]R_g: Radius of gyration of the Gaussian polymer chain

mm^2 and floated in water. One piece was scooped with a chip sensor and placed in the active area. Subsequently, the polymer-mounted chip sensor was dried under vacuum at room temperature for 24 h. PEMA films were also mounted with the procedure described above. The surface of the chip sensor was composed of silica; thus, adsorption occurred at the polymer/silica interface. The time evolution of the storage heat capacity for the mounted polymer film was measured during adsorption with differential AC chip calorimetry. The details of these measurements were described in our previous study [42]. The complex heat capacities of the sample films were measured at $T_g + 50$ K and $T_g + 15$ K under a nitrogen flow of 0.1 mL min^{-1}. The frequency of the temperature modulation was 200 Hz, and the applied AC voltage was 0.3 or 0.8 V, which resulted in a temperature amplitude of approximately 0.14 or 1.1 K, respectively.

AFM observation

The Guiselin approach was used for PtBMA and PEMA to investigate how the surface morphologies of the adsorbed layers changed as adsorption proceeded. Spincast films of the polymers were prepared in the same manner as described above, and pieces of the films (5 × 5 mm^2) were floated in water. Then, the floating films were placed on Si substrates of which the surfaces were covered with native oxide; this surface was the same as that of the chip calorimeter. The resulting films were then annealed at $T_g + 15$ K and $T_g + 50$ K for several different durations. The annealed films were immersed in toluene for 60 min at 40 °C to remove unadsorbed polymer materials. This solvent leaching process was repeated three times. To study the surface morphology of the adsorbed polymer layer, tapping-mode AFM was performed with an E-sweep (Hitachi, Tokyo, Japan). The cantilever tip used for the measurement was microfabricated from Si, and the spring constant and resonance frequency were 13 N m^{-1} and 130 kHz, respectively. The shape of the AFM probe chip was evaluated to correct the lateral sizes in the obtained images. The thicknesses of the adsorbed layers were determined via AFM. The range of the scanning varied from 200 × 200 nm^2 to 10 × 10 μm^2.

Results and discussion

Adsorption kinetics and morphology

We defined the relative degree of adsorption $\gamma(t)$ as

$$\gamma(t) = [C'(0) - C'(t)]/[C'(0) - C'(\infty)] \quad (1)$$

where $C'(t)$ is the storage heat capacity at adsorption time t. As adsorption proceeded, the mobility of the polymer chains near the interface decreased due to anchoring of the segments at the substrate surface; thus, the storage heat capacity decreased as adsorption proceeded. $\gamma(t)$ increased with decreasing $C'(t)$ from zero to unity during adsorption. Figure 1 shows $\gamma(t)$ for PtBMA with respect to the adsorption time at 430 K ($T_g + 50$ K). $\gamma(t)$ increased slowly over a time range of 10^5 s, which was consistent with the typical adsorption behaviors of other polymers [1]. The increase in $\gamma(t)$ was attributed to the melt adsorption

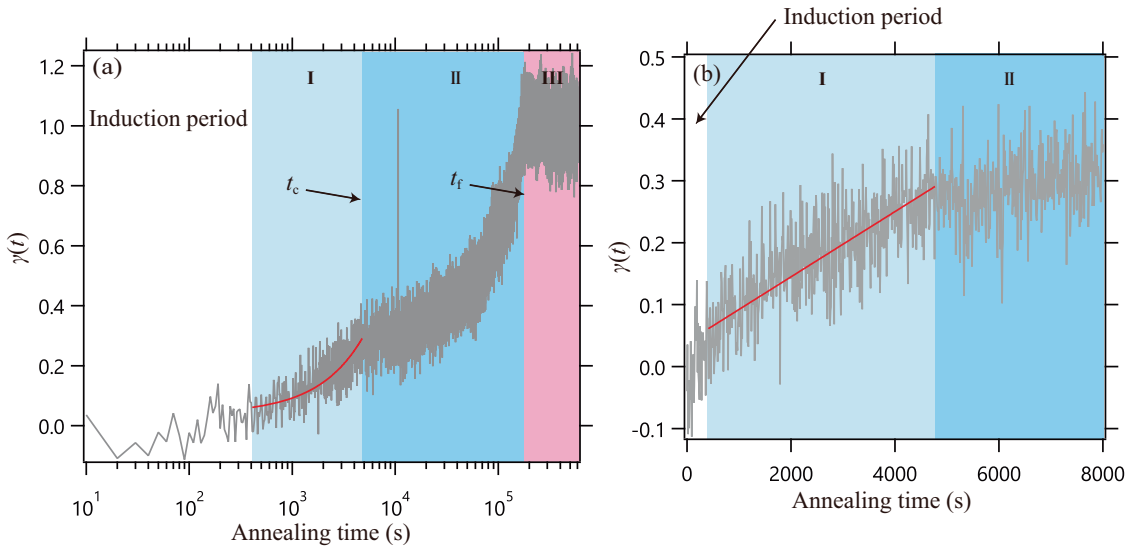

Fig. 1 Time evolution for the degree of adsorption $\gamma(t)$ of PtBMA at 428 K; **a** plotted against logarithmic time, and **b** plotted against time (linear plot) in the initial time region. The solid lines show the result of fitting with Eq. (2). t_c and t_f are the crossover time and the time when adsorption ceased, respectively. The temperature amplitude was ca. 0.14 K

process, and no other significant relaxation processes independent of adsorption on a similar time scale were considered. In Fig. 1, we observed an initial time period before ca. 300 s, during which $\gamma(t)$ fluctuated irregularly and irreproducibly. This may be an induction period, during which some relaxation processes occurred for unstable structures that remained in the spin-cast film. It was assumed that adsorption would be observed after the induction period. We found that the length of the induction period depended on the temperature. We roughly determined the onset time of adsorption, i.e., the end of the induction period, as the starting time of linear growth with t (see Fig. 1b).

After the induction period, the obtained curve exhibited a two-step profile. A two-step profile has generally been observed for polymers such as PS, poly(2-vinylpyridine), and poly(bisphenol A carbonate), which is composed of the first rapid regime (the amount adsorbed increases linearly with time) and the second slow regime (adsorption proceeds with log t) [1, 20, 21]. It was inferred that in the first stage, segments near the vacant sites on the surface were rapidly adsorbed, whereas in the second stage, nonadsorbed chains had to crawl into the already adsorbed chains to find residual vacant sites. We infer that the two-step growth observed for PtBMA may indicate the same mechanism as above. However, the profile in the second stage (regime II) is slightly different from those reported thus far, as described below, and we modified the mechanism in regime II as we discuss later.

The profile in Fig. 1 shows a linear growth region before t_c as indicated by regime I in the figure, and the slope decreased discontinuously at t_c. In the second region, indicated as regime II in Fig. 1, the slope increased continuously with time until the completion of adsorption at t_f. Subsequently, adsorption did not proceed (regime III). The nonlogarithmic increase (associated with the increasing slope) shown in regime II may be characteristic of rigid polymers, such as PtBMA.

To evaluate the adsorption rate quantitatively, the profile of regime I in Fig. 1 was fitted with the following equation:

$$h(t) = h_0 + vt \quad t < t_c \tag{2}$$

where h is the thickness of the adsorbed layer, h_0 is the thickness of the adsorbed layer at $t = 0$, and v is the growth rate before the crossover time t_c [1, 18–21]. The solid curve in Fig. 1 shows the results of the fitting analysis. Table 2 lists the values obtained for t_c, t_f, and v.

Figure 2 shows AFM images of the surfaces of the adsorbed layers of PtBMA obtained via the Guiselin approach. The images indicated that the adsorbed amount increased with annealing time. The sizes of the particles increased from 600 to 1200 s, as shown in Table 3. Considering the radius of gyration R_g for an unperturbed chain

Table 2 Parameters evaluated from the profile of $\gamma(t)$

Polymer	t_c/s	t_f/s	v/s^{-1}
PtBMA ($T_g + 50$ K)	4.7×10^3	1.8×10^5	4.9×10^{-5}
PtBMA ($T_g + 15$ K)	–	4.2×10^4	3.0×10^{-5}
PEMA ($T_g + 50$ K)	4.3×10^3	$>4 \times 10^5$	5.2×10^{-5}

of PtBMA (7.1 nm, as shown in Table 1), we infer that one particle consists of several polymer chains. At $t = 1200$ s, aggregated polymer particles with diameters of approximately 45–210 nm were separated by distances longer than several tens of nanometers. These values of the particle size were obtained by correcting for the shape of the probe chip (the effective width of the chip was found to be 15 and 30 nm at particle heights of 4.4 and 9.2 nm, respectively). This result suggested that the adsorbed polymer chains tended to aggregate into particles during the initial stage. This sporadic morphology for adsorption in the first stage suggested the linear growth of $\gamma(t)$ rather than log t growth as shown in Fig. 1.

At $t = 1800$ s, no particles were discernible and the entire surface appeared to be covered with adsorbed polymers. In addition, a groove-like texture was observed at a depth of approximately 1 nm. As the particles grew, they coalesced, which resulted in bumps and grooves. At $t = 3600$ s, the texture of grooves with a depth of approximately 2.4 nm was more clearly observed. After the completion of adsorption at $t = 1.8 \times 10^5$ s, a sea-island structure was observed. The average thickness of the adsorbed layer was estimated from the AFM images to be 44 nm, which may be rather large compared to the final thicknesses observed for other polymer systems reported to date.

The chip calorimetry and AFM results suggested that the adsorption of PtBMA occurred in two stages. In the first stage, the polymer chains were adsorbed onto the silica substrate with relatively small rearrangements or conformational transitions; only the attachment of segments to the surface occurred, as shown in Fig. 3-I. In this region (regime I), $\gamma(t)$ increased linearly with annealing time, and clusters were formed on the substrate surface as shown by the AFM images in Fig. 2a–c.

We now propose a modified mechanism for adsorption in regime II, although this is just one possible explanation for the result in Fig. 1. In the second stage, the polymer chains undergo large scale movements to reach the residual adsorption sites as shown in Fig. 3-II-1. During this period, the AFM images showed that the adsorbed chains covered the entire surface of the substrate, as seen in Fig. 2d, e. Adsorption at this stage proceeded as the polymer chains far from the interface migrated into the adsorption layer. The adsorption rate was slower than that of the first stage because the process involved large-scale motion. The chains

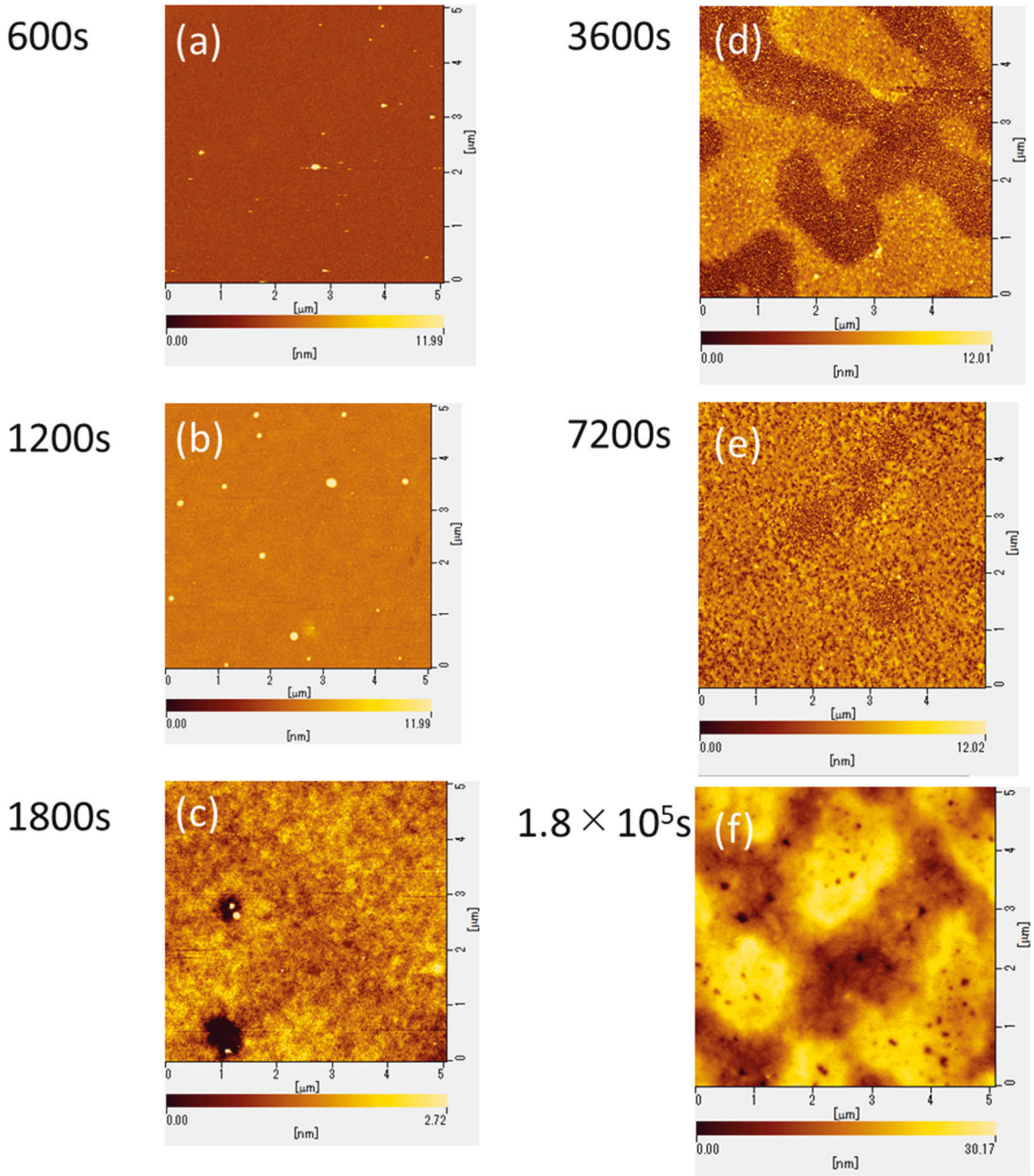

Fig. 2 AFM topographic images of the adsorbed layer of PtBMA obtained via the Guiselin approach at various annealing times. The annealing temperature was 428 K. The scan sizes and height scales of the images for **a**, **b**, **d**, and **e** are 5 × 5 μm^2 and 0−12 nm, respectively. For the images of **c** and **f** taken at $t = 1800$ s and $t = 1.8 \times 10^5$ s, respectively, the scan size was also 5 × 5 μm^2 and height scales of the images were 0−2.7 nm and 0−30 nm, respectively

adsorbed by crawling had tails that remained outside the adsorbed layer, as shown in Fig. 3-II-2. However, these rigid tails (or loops) connected to anchored segments at the surface had lower mobilities than the unadsorbed free chains. These tails with low mobilities interacted via chain entanglements with neighboring segments that belong to other free chains, so that their mobilities were also lowered. Thus, the free chains were dynamically coupled with rigid tails and were incorporated in the adsorption process (indirect adsorption). This indirect adsorption promoted the growth of the low-mobility region (adsorbed layer). This process may be reflected in the increasing slope of $\gamma(t)$ in regime II, as the storage heat capacity was sensitive to the reduction in segmental mobility. The adsorption processes in regime II continued until further entanglement of the adsorbed chains ceased.

Simulation studies revealed that the end-to-end distances of adsorbed chains attached to a surface tended to increase

as the adsorption energy increased [44, 45]. PtBMA is considered to undergo a strong adsorption on the silica surface (native oxide) because of its ester linkages, which interact strongly with the silica surface via hydrogen bonding [46]. Thus, the PtBMA chains near the interface may tend to assume more extended conformations than unperturbed chains. On the other hand, this interfacial effect on the chain conformation may be weaker for PS with fewer polarized groups. As a result, the increasing slope in regime II was not prominent for PS, and the growth proportional to log t was observed [1].

Table 3 Results from analysis of the AFM images of PtBMA and PEMA

Polymer	Annealing time/s	Area per particle/μm^2	Number density of particles/μm^{-2}
PtBMA	600	8.9×10^{-2}	6
PtBMA	1200	1.3×10^{-1}	6
PEMA	600	8.4×10^{-4}	225
PEMA	1200	6.2×10^{-4}	343
PEMA	3600	1.2×10^{-4}	163

Figure 4 shows the $\gamma(t)$ results for PtBMA annealed at $T_g + 15$ K. In this case, a single-step profile was observed. The solid curve in Fig. 4 shows the result of the fit with Eq. 2, and the adsorption process is considered to occur in regime I. This suggested that loose adsorption with crawling did not occur because of the reduced mobility of the polymer chains at lower temperatures. It should be noted that the v for PtBMA depended on the annealing temperature: v increased with increasing temperature. This result is consistent with those reported previously [1, 18, 47].

Figure 5 shows the calorimetric results obtained for PEMA at 399 K ($T_g + 50$ K). The profile of $\gamma(t)$ was similar to that of PtBMA at $T_g + 50$ K: a linear growth regime occurred in the first stage, followed by a slower growth

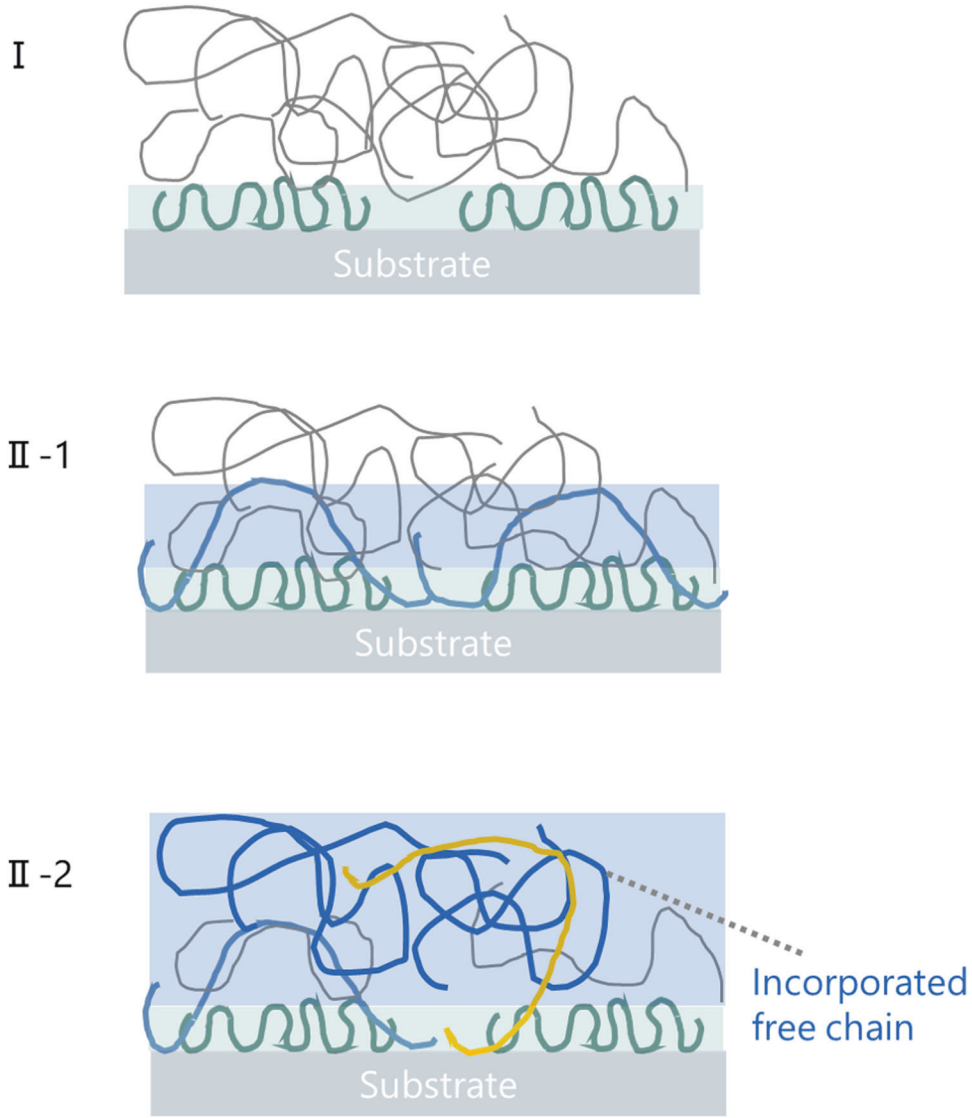

Fig. 3 Schematic illustrations of the time evolution for the adsorbed chains

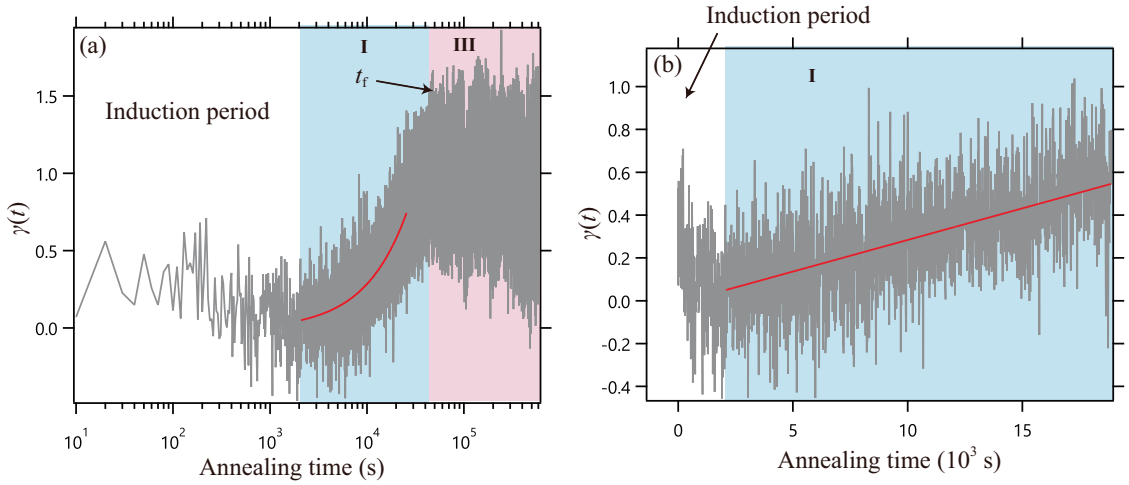

Fig. 4 Time evolution of the degree of PtBMA adsorption $\gamma(t)$ at 395 K; **a** plotted against logarithmic time, and **b** plotted against time (linear plot) in the initial time region. The solid lines show the result of fitting with Eq. (2). t_f is the time at which adsorption ceased. The temperature amplitude was ca. 0.14 K

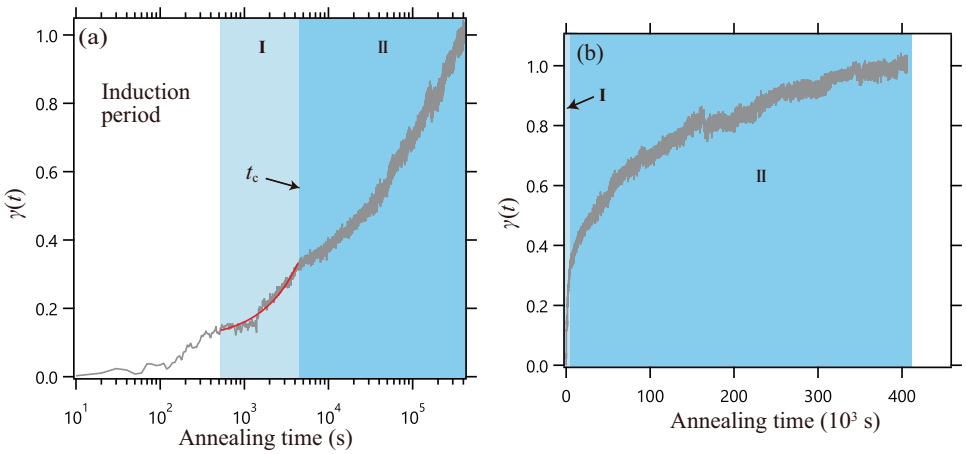

Fig. 5 Time evolution of the degree of PEMA adsorption $\gamma(t)$ at 399 K; **a** plotted against logarithmic time, and **b** plotted against time (linear plot) over the whole range of time. The solid line shows the result of fitting with Eq. (2). The temperature amplitude was ca. 1.1 K

regime in which the growth rate gradually increased. Noticeably, we did not observe completion of adsorption within our experimental time range (<4 × 10^5 s), although the linear plot with respect to time (Fig. 5b) suggested that $\gamma(t)$ nearly reached the final value at 4 × 10^5 s. Anyhow, PEMA exhibited a longer t_f value than PtBMA (see Table 2). This suggested that adsorption continued beyond the measurement time range (>4 × 10^5 s).

Figure 6 shows AFM images of the surfaces of the adsorbed PEMA layers prepared via the Guiselin approach. Small particles of aggregated polymer molecules were observed at annealing times from 600 s to 1.8 × 10^5 s. In particular, after annealing for 600 and 3600 s, only particles were observed; otherwise, the bare surface of the substrate was exposed. The particles grew gradually as adsorption proceeded. The average size and number density of the particles were evaluated and are listed in Table 3.

Comparison of PtBMA and PEMA

We now discuss the differences in the adsorption behaviors of PtBMA and PEMA. Table 2 lists the values of v obtained from fitting with Eq. (2), as well as the t_c and t_f values. These polymers exhibited similar two-step $\gamma(t)$ profiles, as shown in Figs. 2 and 5. In Regime II, the slope tended to increase with time. This tendency was more prominent for PtBMA than for PEMA. This result may reflect difference in the chain conformations near the interface as discussed in the previous section. In addition, the difference in chain rigidity (stiffness) might be related to the adsorption behavior. The static chain stiffness parameter λ^{-1} for poly(isopropyl methacrylate) was reported to be much greater than that for PEMA [48]. PtBMA has bulkier side groups than poly(isopropyl methacrylate). Therefore, PtBMA is considered to be stiffer than PEMA. It should also be noted that the value of λ^{-1} for PS is lower than that for PEMA, irrespective of the stereoregularity [49].

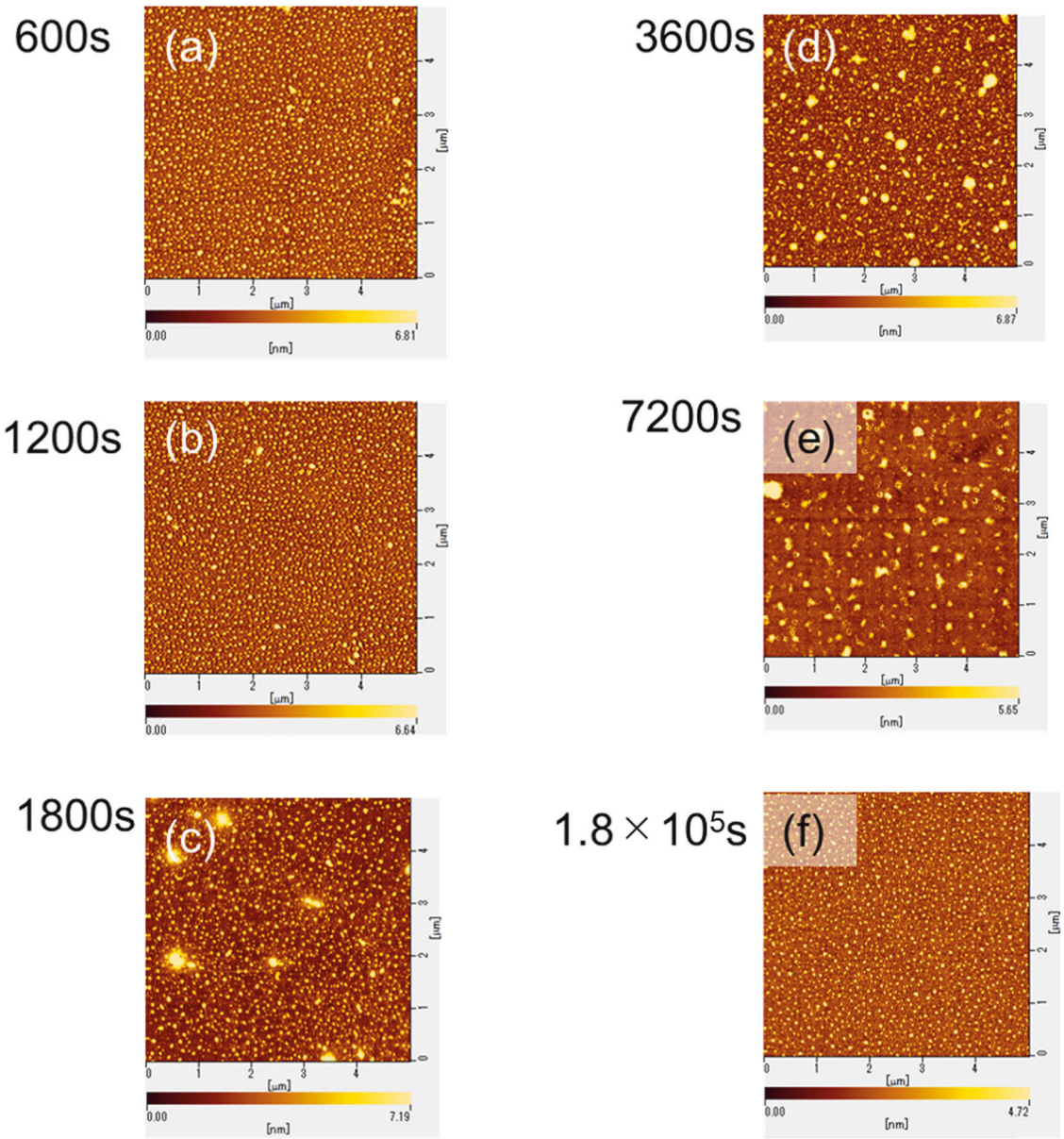

Fig. 6 AFM topographic images of the adsorbed layer of PEMA obtained from the Guiselin approach at various annealing times. The annealing temperature was 399 K. The scan sizes and height scales of the images are 5×5 μm^2 and $0 - 7.2$ nm, respectively

However, poly(adamantyl methacrylate), which carries even bulkier side groups, showed a weaker tendency of increasing slope in regime II. The results are shown in the Supplementary Information.

Several factors affect the adsorption process, such as the molecular weight [1, 18, 19], annealing temperature, polymer/substrate interactions, polarity [22], and rigidity of the polymer chain. Herein, we focus on the adsorption process in regime I, which is characterized by t_c and v. At $T_g + 50$ K, the values of t_c and v did not differ significantly, as shown in Table 2. Note that the difference in the chemical structures of PtBMA and PEMA may not be significant, whereas their molecular weights differ, as shown in Table 1. Housmans et. al. reported that t_c was independent of the molecular weight [18], whereas other researchers found that t_c depended on the molecular weight. Nevertheless, the present results suggest that differences in the chemical structure and chain rigidity did not significantly affect adsorption in regime I.

We determined the values of t_f for PtBMA within our experimental time range. In contrast, t_f was not observed for PEMA at $T_g + 50$ K until 4×10^5 s. In our previous study, the adsorption kinetics of poly(9-anthracenyl methyl methacrylate), which carries bulky side groups, did not show any plateau even after 7.0×10^5 s [42]. Furthermore, Gawek et al. reported unexpected results for poly(vinyl acetate): t_f was found to be 2.6×10^5 s at $T_g + 32$ K, while at

$T_g + 42$ K, t_f was not observed even after 1.1×10^6 s despite a small temperature difference of 10 K [20]. They found that structural changes accompanied by diffusion of the polymer chains occurred above a specific temperature. Similarly, the adsorption of methacrylate polymers may have a strong temperature dependence.

Conclusion

In this study, we investigated the adsorption kinetics and morphologies of the adsorbed layers of PtBMA and PEMA with AC chip calorimetry and AFM. The $\gamma(t)$ results revealed two-step profiles for both polymers. In the first step (regime I), $\gamma(t)$ grew linearly with time, and in the second step (regime II), the slope gradually increased with log t. The feature of an increasing slope in the latter step has not been reported for other polymers, such as PS, which showed a linearly increasing profile with log t. The tendency of the slope to increase in regime II was more prominent for PtBMA than for PEMA. This may reflect differences in the chain mobilities or rigidities of the two polymers. Furthermore, a remarkable result is that the adsorption layer grew up to 44 nm, which was larger than those reported previously for typical systems such as PS. These findings suggested that in the region near the interface, free chains that were not directly adsorbed at the interface were incorporated into the adsorption layer via interactions with the adsorbed chains, and as a result, the adsorption process was further promoted. We also found that the exposed adsorbed layers for PtBMA and PEMA showed different morphologies: PtBMA exhibited heterogeneous bumps and grooves after an adsorption time of 1800 s, whereas PEMA showed small particles throughout the adsorption process. Furthermore, the adsorption kinetics depended strongly on the annealing temperature. PtBMA annealed at $T_g + 15$ K showed only a linear growth regime, in contrast to the profile at $T_g + 50$ K. Further investigation is required for various polymers over a wider range of annealing temperatures to elucidate the relationship between polymer structures and adsorption kinetics. These results provide new insights into nonequilibrium interfacial phenomena.

Acknowledgements This study was supported by JSPS KAKENHI Grant Numbers JP20K05615 and JP23K04853 from the Ministry of Education, Culture, Sports, Science, and Technology of Japan.

Funding Open Access funding provided by University of Fukui.

Compliance with ethical standards

Conflict of interest The authors declare no competing interests.

References

1. Napolitano S, Wübbenhorst M. The lifetime of the deviations from bulk behaviour in polymers confined at the nanoscale. Nat Commun. 2011;2:260.
2. Spiece J, Martinez-Tong DE, Sferrazza M, Nogales A, Napolitano S. Are polymers glassier upon confinement? Soft Matter. 2015;1:6179–86.
3. Burroughs MJ, Napolitano S, Cangialosi D, Priestley RD. Direct measurement of interfacial effects on exposed and buried adsorbed nanolayer glass transition temperature in polymer thin films. Macromolecules. 2016;49:4647–55.
4. Napolitano S. Irreversible adsorption of polymer melts and nanoconfinement effects. Soft Matter. 2020;16:5348.
5. Koga T, Jiang N, Gin P, Endoh MK, Narayanan S, Lurio LB, et al. Impact of an irreversibly adsorbed layer on local viscosity of nanoconfined polymer melts. Phys Rev Lett 2011;107:225901.
6. He Q, Narayanan S, Wu DT, Foster MD. Confinement effects with molten thin cyclic polystyrene films. ACS Macro Lett. 2016;5:999–1003.
7. Asada M, Jiang N, Sendogdular L, Sokolov J, Endoh MK, Koga T, et al. Melt crystallization/dewetting of ultrathin PEO films via carbon dioxide annealing: the effects of polymer adsorbed layers. Soft Matter. 2014;10:6392–403.
8. Unni AB, Vignaud G, Bal JK, Delorme N, Beuvier T, Thomas S, et al. Solvent assisted rinsing: stability/instability of ultrathin polymer residual layer. Macromolecules. 2016;49:1807–15.
9. Jiang N, Cheung JM, Guo Y, Endoh MK, Koga T, Yuan G, et al. Stability of adsorbed polystyrene nanolayers on silicon substrates. Macromol Chem Phys. 2018;219:1700326.
10. Braatz ML, Melendez LI, Sferrazza M, Napolitano S. Unexpected impact of irreversible adsorption on thermal expansion: Adsorbed layers are not that dead. J Chem Phys. 2017;146:203304.
11. Vanroy B, Wubbenhorst M, Napolitano S. Crystallization of thin polymer layers confined between two adsorbing walls. ACS Macro Lett. 2013;2:168–72.
12. Martinez-Tong DE, Vanroy B, Wübbenhorst M, Nogales A, Napolitano S. Crystallization of poly(l-lactide) confined in ultrathin films: Competition between finite size effects and irreversible chain adsorption. Macromolecules. 2014;47:2354–60.
13. Jeong H, Napolitano S, Craig BA, Priestley RD. Irreversible adsorption controls crystallization in vapor-deposited polymer thin films. J Phys Chem Lett. 2017;8:229–34.
14. Jenckel E, Rumbach B. Über die Adsorption von hochmolekularen Stoffen aus der Lösung. Angew Phys Chem. 1951;55:612–18.
15. Guiselin O. Irreversible adsorption of a concentrated polymer solution. Europhys Lett. 1991;17:225.

16. Gin P, Jiang N, Liang C, Taniguchi T, Akgun B, Satija SK, et al. Revealed architectures of adsorbed polymer chains at solid-polymer melt interfaces. Phys Rev Lett. 2012;109:265501.
17. Jiang N, Shang J, Di X, Endoh MK, Koga T. Formation mechanism of high-density, flattened polymer nanolayers adsorbed on planar solids. Macromolecules. 2014;47:2682–9.
18. Housmans C, Sferrazza M, Napolitano S. Kinetics of irreversible chain adsorption. Macromolecules. 2014;47:3390–93.
19. Thees MF, McGuire JA, Roth CB. Review and reproducibility of forming adsorbed layers from solvent washing of melt annealed films. Soft Matter. 2020;16:5366–87.
20. Gawek M, Omar H, Szymoniak P, Schönhals A. Growth kinetics of the adsorbed layer of poly(2-vinylpyridine) – an indirect observation of desorption of polymers from substrates. Soft Matter. 2023;19:3975–82.
21. Omar H, Hidde G, Szymoniak P, Hertwig A, Schönhals A. Growth kinetics of the adsorbed layer of poly(bisphenol A carbonate) and its effect on the glass transition behavior in thin films. RSC Adv. 2023;13:14473–83.
22. Davis MJB, Zuo B, Priestley RD. Competing polymer–substrate interactions mitigate random copolymer adsorption. Soft Matter. 2018;14:7204–13.
23. Sharma T, Konishi M, Sekiya K, Takahashi I. Thickness and substrate dependences of the relaxation of spin coated polymethyl methacrylate ultrathin films supported on SiO_2 and SiOH substrates. Macromolecules. 2021;54:2637–46.
24. Monnier X, Napolitano S, Cangialosi D. Direct observation of desorption of a melt of long polymer chains. Nat Commun 2020;11:4354.
25. Fujii Y, Yang Z, Leach J, Atarashi H, Tanaka K, Tsui OKC. Affinity of polystyrene Films to hydrogen-passivated silicon and its relevance to the T_g of the films. Macromolecules. 2009;42:7418–22.
26. Kremer K. Glassy states of adsorbed flexible polymers and spread polymer monolayers. J Phys France. 1986;47:1269–71.
27. Frantz P, Granick S. Kinetics of polymer adsorption and desorption. Phys Rev Lett. 1991;66:899–902.
28. Schneider HM, Granick S. Kinetic traps in polymer adsorption: exchange of polystyrene between the adsorbed state and a good solvent. Macromolecules. 1992;25:5054–9.
29. Frantz P, Granick S. Exchange kinetics of adsorbed polymer and the achievement of conformational equilibrium. Macromolecules. 1994;27:2553–8.
30. Priestley RD, Cangialosi D, Napolitano S. On the equivalence between the thermodynamic and dynamic measurements of the glass transition in confined polymers. J Non-Cryst Solids. 2015;407:288–95.
31. Jiang N, Sendogdular L, Di X, Sen M, Gin P, Endoh MK, et al. Effect of CO_2 on a mobility gradient of polymer chains near an impenetrable solid. Macromolecules. 2015;48:1795–803.
32. Xu J, Zhang Y, Zhou H, Hong Y, Zuo B, Wang X, et al. Probing the utmost distance of polymer dynamics suppression by a substrate by investigating the diffusion of fluorinated tracer-labeled polymer chains. Macromolecules. 2017;50:5905–13.
33. Koga T, Barkley D, Nagao M, Taniguchi T, Carrillo JMY, Sumpter BG, et al. Interphase structures and dynamics near nanofiller surfaces in polymer solutions. Macromolecules. 2018;51:9462–70.
34. Zuo B, Zhou H, Davis MJ, Wang X, Priestley RD. Effect of local chain conformation in adsorbed nanolayers on confined polymer molecular mobility. Phys Rev Lett. 2019;122:217801.
35. Park H, Lee SH. Review on interfacial bonding mechanism of functional polymer coating on glass in atomistic modeling perspective. Polymers. 2021;13:2244.
36. Huang J, Zhou J, Liu M. Interphase in polymer nanocomposites. ACS Au. 2022;2:280–91.
37. Tian H, Bi C, Li Z, Wang C, Zuo B. Metastable polymer adsorption dictates the dynamical gradients at interfaces. Macromolecules. 2023;56:4346–53.
38. Simavilla DN, Panagopoulou A, Napolitano S. Characterization of adsorbed polymer layers: preparation, determination of the adsorbed amount and investigation of the kinetics of irreversible adsorption. Macromol Chem Phys. 2018;219:1–6.
39. Sen M, Jiang N, Cheung J, Endoh MK, Koga T, Kawaguchi D, et al. Flattening process of polymer chains irreversibly adsorbed on a solid. ACS Macro Lett. 2016;5:504–8.
40. Simavilla DN, Huang W, Vandestrick P, Ryckaert JP, Sferrazza M, Napolitano S. Mechanisms of polymer adsorption onto solid substrates. ACS Macro Lett. 2017;6:975–9.
41. Simavilla DN, Huang W, Housmans C, Sferrazza M, Napolitano S. Taming the strength of interfacial interactions via nanoconfinement. ACS Cent Sci. 2018;4:755–9.
42. Ishihara M, Watanabe T, Sasaki T. Adsorption kinetics of polystyrene and poly(9-anthracenyl methyl methacrylate) onto SiO_2 surface measured by chip nano-calorimetry. Polymers. 2022;14:605.
43. Yin H, Madkour S, Schönhals A. Unambiguous evidence for a highly mobile surface layer in ultrathin polymer films by specific heat spectroscopy on blends. Macromolecules. 2015;48:4936–41.
44. Mark P, Windwer S. Polymer adsorption on a surface by an exact enumeration study. Macromolecules. 1974;7:690–697.
45. Torrie GM, Middlemiss KM, Bly SHP, Whittington SG. Self-avoiding walks interacting with an interface. J Chem Phys. 1976;65:1867–1871.
46. Kawaguchi D, Sasahara K, Inutsuka M, Abe T, Yamamoto S, Tanaka K. Absolute local conformation of poly(methyl methacrylate) chains adsorbed on a quartz surface. J Chem Phys. 2023;159:244902.
47. Yu C, Granick S. Revisiting polymer surface diffusion in the extreme case of strong adsorption. Langmuir. 2014;30:14538–44.
48. Sasaki T, Arisawa H, Yamamoto M. Fluorescence depolarization study on local motions of anthracene-labeled poly(alkyl methacrylate)s in dilute solutions and evaluation of their chain stiffness. Polym J. 1991;23:103–115.
49. Yamakawa H. A hypothesis on polymer chain configurations. Helical wormlike chains. Macromolecules. 1977;10:692–696.